

Fig. 10. Photograph of trial type CRI670-2 filter.

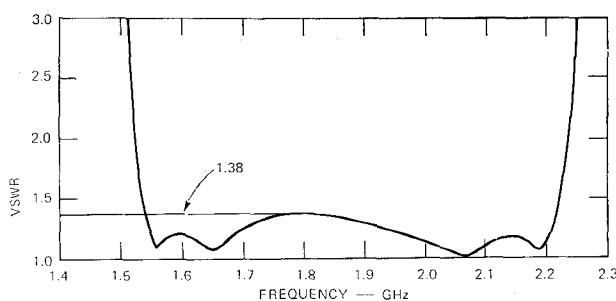


Fig. 11. Measured VSWR of trial type CRI670-2 filter.

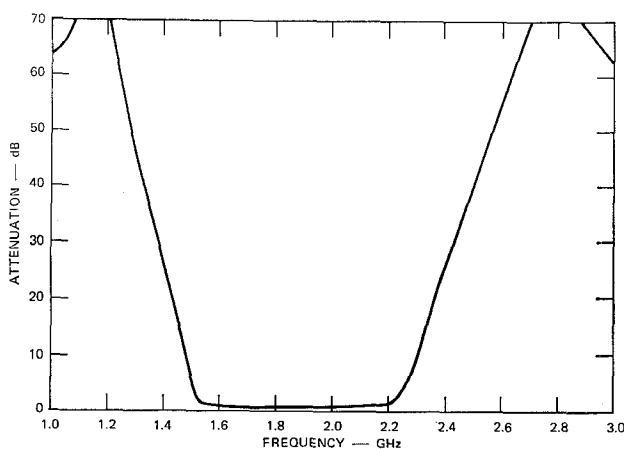


Fig. 12. Measured attenuation of trial type CRI670-2 filter.

quency was set at 2.0 GHz and both poles of attenuation were set to 1.2 GHz. A photograph of the constructed filter is shown in Fig. 8. Its calculated and measured VSWR and attenuation responses are shown in Figs. 9(a) and (b), respectively. The measured VSWR was found somewhat high, particularly near midband. This was determined to be the result of insufficient coupling of the input and output resonators. A slight increase in the coupling of the first and last pairs of coupled lines would have improved the response. The calculated and measured attenuation responses agreed very well after accounting for the slight shift in center frequency.

A photograph of an interdigital realization for this class of filter is shown in Fig. 10. The specifications for this trial design were the same as in the previous case. The dimensions for the coupled-line array were realized with the data of Cristal [5]. The ground plane spacing was 0.350 in. The uncoupled stubs were constructed of dielectric loaded coaxial lines that were short circuited at their ends with an adjustable tuning slug. The measured VSWR after tuning is shown in Fig. 11. Although the tuning was not optimum (2 points of match are suppressed), the peak VSWR was only 1.38 compared to the theoretical value of 1.36. The measured attenuation response is shown in Fig. 12. In this case the bandwidth measured about 37 percent compared to the design value of 40 percent. But in general the experimental results compared favorably with the theory.

The filter geometries are believed to be new. However, their

electrical circuits (or duals) are equivalent to the electrical circuit of a filter presented by Mattheai [6] for the particular case of commensurate length lines.

CONCLUSIONS

A new class of microwave wide-band bandpass filters, their design equations, and equivalent circuits, has been presented. The construction of two trial filters demonstrated the practicality of designs for printed circuit and interdigital air line. The experimental data adequately confirmed the design theory.

REFERENCES

- [1] G. L. Mattheai, L. Young, and E. M. T. Jones, *Design of Microwave Filters, Impedance-Matching Networks, and Coupling Structures*. New York: McGraw-Hill, 1964, ch. 4.
- [2] S. B. Cohn, "Shielded coupled-strip transmission lines," *IRE Trans. Microwave Theory Tech.*, vol. MTT-3, pp. 29-38, Oct. 1955.
- [3] J. P. Shelton, Jr., "Impedance of offset parallel-coupled strip transmission lines," *IEEE Trans. Microwave Theory Tech.*, vol. MTT-14, pp. 7-15, Jan. 1966.
- [4] W. J. Getzinger, "Coupled rectangular bars between parallel plates," *IRE Trans. Microwave Theory Tech.*, vol. MTT-10, pp. 65-72, Jan. 1962.
- [5] E. G. Cristal, "Coupled circular cylindrical rods between parallel ground planes," *IRE Trans. Microwave Theory Tech.*, vol. MTT-12, pp. 428-439, July 1964.
- [6] G. L. Mattheai, "Design of wide-band (and narrow-band) band-pass microwave filters on the insertion loss basis," *IEEE Trans. Microwave Theory Tech.*, vol. MTT-8, pp. 580-593, Nov. 1960; see Fig. 3.

An Approximate Analysis of Dielectric-Ridge Loaded Waveguide

R. M. ARNOLD AND F. J. ROSENBAUM

Abstract—The dielectric-ridge loaded waveguide is analyzed approximately in terms of coupled empty waveguide modes. Using this technique the propagation constant can be easily computed, thus allowing the prediction of the properties of a type of dielectric phase shifter.

Experimental evidence is presented which indicates that a two-mode approximation yields reasonable accuracy if the dielectric ridge is on center, is relatively thin compared to the width of the waveguide, and has a low dielectric constant relative to that of free space ϵ_0 .

INTRODUCTION

A common type of variable waveguide attenuator or phase shifter consists of a vane of dielectric material extending into the waveguide through a slot in the broad wall. This type of structure tends to couple many of the normal modes of the waveguide and is consequently difficult to analyze exactly. It is the purpose of this short paper to outline a simple analytical approach to this problem, considering the coupling of only two modes, and compare the results with experiment.

ANALYSIS

Hord and Rosenbaum [1] have described the application of Schelkunoff's generalized telegraphists' equations [2] to isotropic lossless waveguides. This technique involves the expansion of the fields in a loaded waveguide in terms of the normal modes of the empty waveguide. The coefficients of the terms in the linear expansion are determined by the coupling of the empty waveguide modes by the loading. In principle, an infinite number of modes yields an exact solution, but useful approximations can be obtained by considering only the coupling of the most important modes. These most strongly coupled modes are a function of the geometry of the loading. Since the result of the analysis is a polynomial expression in the propagation constant, of order $2N$, where N is the number of modes considered, the fewer important modes coupled, the simpler the analytical problem becomes.

MODE COUPLING

The geometry under consideration is shown in Fig. 1. Assume that ϵ_1 describes a loss free medium with $\epsilon_1 > \epsilon_0$. The concentration of fields in the x dimension, in general, gives rise to a transverse variation proportional to $\sum_{n=1}^{\infty} \sin n\pi x/a$, where n is odd for center

Manuscript received November 5, 1971; revised February 22, 1972.

R. M. Arnold is with Bell Laboratories, Columbus, Ohio 43212.

F. J. Rosenbaum is with the Department of Electrical Engineering, Washington University, St. Louis, Mo. 63130.

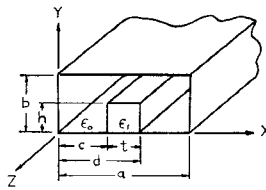


Fig. 1. Geometry of partially loaded waveguide.

loading. The presence of the lateral surface on top of the dielectric, where polarization-induced surface charge exists, will necessarily couple TM modes to the dominant TE_{10} empty waveguide mode. The lowest order TM mode (TM_{11}), at least, should thus be included when $h < b$ [3].

The present analysis is restricted to the solution of a biquadratic equation in the propagation constant (2 modes). The TE_{10} and TM_{11} empty waveguide modes will be important and we consider only the case where higher order TE modes do not unduly influence the propagation. This will be valid when one or more of the following conditions exists with the dielectric centrally located in the x dimension: 1) $\epsilon_1 \approx \epsilon_0$; 2) $t \ll a$; 3) $t \approx a$. The vane-type dielectric phase shifter problem under consideration satisfies condition 2) above.

ANALYSIS

The results presented here are obtained by integrating combinations of scalar mode functions and loading material parameters over four regions in the waveguide cross section: two areas $[(a-t)/2] \times b$, one $t \times (b-h)$, and one $t \times h$. The details of this procedure are given more fully in [1] and [3]. The propagation constant $\Gamma = \alpha + j\beta$ (here $\alpha = 0$) is given by the roots of the following equations:

$$\Gamma^4 - \Gamma^2(BF - GH) - (GBFH - GA^2F) = 0 \quad (1)$$

where

$$\begin{aligned} A &= K_3 \\ B &= -K_1 - K_2 \\ F &= -K_5 - K_6 - \frac{X_{(11)}}{K_{12}} \\ G &= K_{13} \\ H &= -K_7 - \frac{X_{(10)}}{K_9} \\ K_{(10)} &= \frac{\pi}{a} \\ X_{(11)} &= \sqrt{\frac{\pi^2}{a^2} + \frac{\pi^2}{b^2}} \end{aligned} \quad (2)$$

and

$$\begin{aligned} K_1 &= \frac{j\omega\epsilon_0}{1 + \left(\frac{a}{b}\right)^2} \left\{ 1 + \left(\frac{\epsilon_1}{\epsilon_0} - 1\right) \left(\frac{t}{a} - \frac{1}{\pi} \sin \frac{\pi t}{a} \right) \left(\frac{h}{b} - \frac{1}{2\pi} \sin \frac{2\pi h}{b} \right) \right\} \\ K_2 &= \frac{j\omega\epsilon_0}{1 + \left(\frac{b}{a}\right)^2} \left\{ 1 + \left(\frac{\epsilon_1}{\epsilon_0} - 1\right) \left(\frac{t}{a} + \frac{1}{\pi} \sin \frac{\pi t}{a} \right) \left(\frac{h}{b} + \frac{1}{2\pi} \sin \frac{2\pi h}{b} \right) \right\} \\ K_3 &= \frac{\sqrt{2j\omega\epsilon_0}}{\sqrt{1 + \left(\frac{b}{a}\right)^2}} \left(1 - \frac{\epsilon_1}{\epsilon_0} \right) \left(\frac{1}{\pi} \sin \frac{\pi t}{a} \right) \left(\frac{t}{a} + \frac{1}{\pi} \sin \frac{\pi t}{a} \right) \\ K_5 &= \frac{j\omega\mu_0}{1 + \left(\frac{b}{a}\right)^2} \\ K_6 &= \frac{j\omega\mu_0}{1 + \left(\frac{a}{b}\right)^2} \\ K_7 &= j\omega\epsilon_0 \left\{ 1 + \frac{h}{b} \left(\frac{\epsilon_1}{\epsilon_0} - 1 \right) \left(\frac{t}{a} + \frac{1}{\pi} \sin \frac{\pi t}{a} \right) \right\} \end{aligned}$$

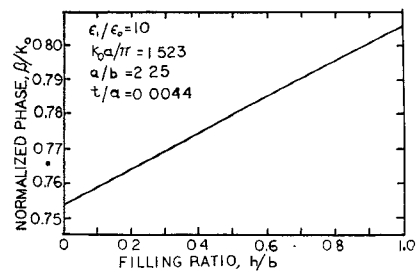


Fig. 2. Normalized phase as a function of filling ratio.

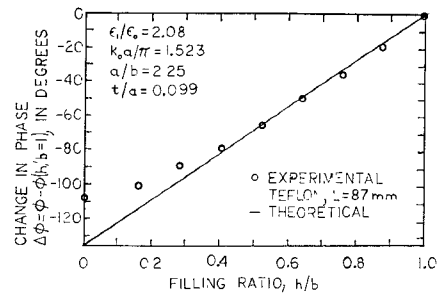


Fig. 3. Comparison of theory and experiment phase shift versus filling ratio.

$$K_9 = j\omega\mu_0 \chi_{(10)} \frac{a^2}{\pi^2}$$

$$\begin{aligned} K_{12} &= \frac{j\omega\epsilon_0 \chi_{(11)}}{\pi^2 \left(\frac{1}{a^2} + \frac{1}{b^2} \right)} \\ &\cdot \left\{ 1 + \left(\frac{\epsilon_1}{\epsilon_0} - 1 \right) \left(\frac{t}{a} + \frac{1}{\pi} \sin \frac{\pi t}{a} \right) \left(\frac{h}{b} - \frac{1}{2\pi} \sin \frac{2\pi h}{b} \right) \right\}. \end{aligned} \quad (3)$$

The reason C , D , and E are absent from (2) and K_4 , K_8 , K_{10} , and K_{11} from (3) is to keep the notation consistent with that used in [3], where terms due to anisotropies in the loading material are included.

It should be noted that when $h \rightarrow b$, (1) yields

$$-\Gamma^2 = k_0^2 + k_0^2 \left(\frac{\epsilon_1}{\epsilon_0} - 1 \right) \left(\frac{t}{a} + \frac{1}{\pi} \sin \frac{\pi t}{a} - \frac{\pi^2}{a^2} \right) \quad (4)$$

where $t = d - c$ (center loading) and $k_0^2 = \omega^2 \epsilon_0 \mu_0$ (ω = radian frequency). This result is the single-mode Rayleigh-Ritz solution and occurs when, in this case, the TE_{10} and TM_{11} modes decouple in the Schelkunoff formulation. The accuracy of (4) has been discussed by Sheikh and Gunn [4].

RESULTS

The results presented in this section were obtained by substituting (2) and (3) into (1) and solving (1) for $\Gamma = j\beta$, the propagation constant. This was done using a computer and the parameter values shown in the figures.

Fig. 2 shows a typical plot of phase (β) versus filling (h/b) for a thin high-dielectric-constant material. If a vane of this material were slowly inserted into the waveguide, the increasing phase shift would be measured with respect to the phase constant (β) at $h/b=0$. The linear change in phase shift is typical of the two-mode Schelkunoff approximation for thin dielectric ridges.

Fig. 3 is a plot of phase shift against h/b for a somewhat thicker but lower dielectric-constant material. Experimental data are also included, with Teflon as the dielectric. The phase shift is referenced here to the $h/b=1$ position since full filling is more exactly defined in the experiment. The theoretical phase shift was obtained from the phase constant β and the sample length L . No account was taken of any effects which could result from the finite sample length [5].

Since the material extended into the waveguide through a slot in the broad wall, when $h/b=0$ there is still the slight influence of a dielectric filled slot in the guide wall, perturbing the propagation. The phase shift is presented in degrees rather than radians. The fit

is quite good for $h/b \geq 0.4$, but the data curve and deviate at low filling.

The curvature in the experimental data can be explained by the presence of higher order modes not considered in the analysis. These modes would be expected to have more influence for thicker and higher dielectric-constant loads. The Teflon dielectric, while rather thick, had a relatively low dielectric constant. An experiment with a glass slab, having a relatively higher dielectric constant and being relatively thick, showed the same trend but exhibited even more curvature. Deviations from theory, especially at low filling, may also be due to the slot through which the dielectric entered the waveguide. This would influence the propagation even when the top of the dielectric was flush with the waveguide wall, and thus, experimentally, $h/b = 0$ does not truly represent the empty waveguide.

SUMMARY

A simple two-mode approximation is presented for the computation of the phase shift of a vane-type dielectric loaded waveguide. This analysis considered the coupling of the TE_{10} and TM_{11} empty waveguide modes by the dielectric. Experimental results tended to support the conclusion that the two-mode analysis is adequate for relatively thin and relatively low dielectric-constant loads centered in the waveguide. The formulation given in (3) can be used to calculate the propagation constant for off-center loads [6] also. However, the accuracy of a two-mode solution using the TE_{10} and TM_{11} modes could be expected to deteriorate rapidly as the load moved off center and other modes became important. A lossy dielectric slab such as used in vane-type attenuators can also be accommodated by this analysis [3].

REFERENCES

- [1] W. E. Hord and F. J. Rosenbaum, "Approximation technique for dielectric loaded waveguides," *IEEE Trans. Microwave Theory Tech.*, vol. MTT-16, pp. 228-233, Apr. 1968.
- [2] S. A. Schelkunoff, "Generalized telegraphists' equations for waveguides," *Bell Syst. Tech. J.*, vol. 31, pp. 784-801, July 1952.
- [3] R. M. Arnold and F. J. Rosenbaum, "Nonreciprocal wave propagation in semiconductor loaded waveguides in the presence of a transverse magnetic field," *IEEE Trans. Microwave Theory Tech.*, vol. MTT-19, pp. 57-65, Jan. 1971.
- [4] R. H. Sheikh and M. W. Gunn, "Wave propagation in a rectangular waveguide inhomogeneously filled with semiconductors," *IEEE Trans. Microwave Theory Tech.*, (Corresp.), vol. MTT-16, pp. 117-121, Feb. 1968.
- [5] S. C. Kashyap and M. A. K. Hamid, "Perturbation analysis in dielectric loaded waveguides," *Electron. Lett.*, vol. 5, pp. 140-141, Apr. 3, 1969.
- [6] A. S. Vander Vorst, A. A. Laloux, and R. J. M. Govaerts, "A computer optimization of the Raleigh-Ritz method," *IEEE Trans. Microwave Theory Tech.*, vol. MTT-17, pp. 454-460, Aug. 1969.

A Single-Tuned Oscillator Circuit for Gunn Diode Characterizations

P. W. DORMAN

Abstract—A Gunn diode oscillator circuit with predictable performance has been developed based on a concept already shown to be practical with IMPATT diodes. Frequency jumps, multifrequency output, and tuning difficulties are eliminated without sacrificing circuit efficiency. The circuit is quite versatile and well suited for Gunn diode characterizations.

An oscillator circuit first developed for X-band IMPATT diode characterization [1] has been adapted for use with Gunn diodes. The predictable single-tuned type of behavior obtained with IMPATT diodes [2], [3] has now been achieved with Gunn diodes as well without sacrificing circuit efficiency. This short paper reports the circuit configuration.

The Gunn oscillator circuit is illustrated in Fig. 1. The diode is mounted in the center conductor of a coaxial transmission line which is coupled to the side wall of a $\lambda_g/2$ waveguide cavity. This coaxial line is terminated in its characteristic impedance beyond the cavity. A $\lambda/4$ series choke is included between the cavity and termination to minimize power leakage into the termination. The external load is coupled to the cavity by a rotary joint-iris combination that allows smooth coupling variation between a value dictated by the iris dimensions and zero coupling. Mode suppressors are located on the

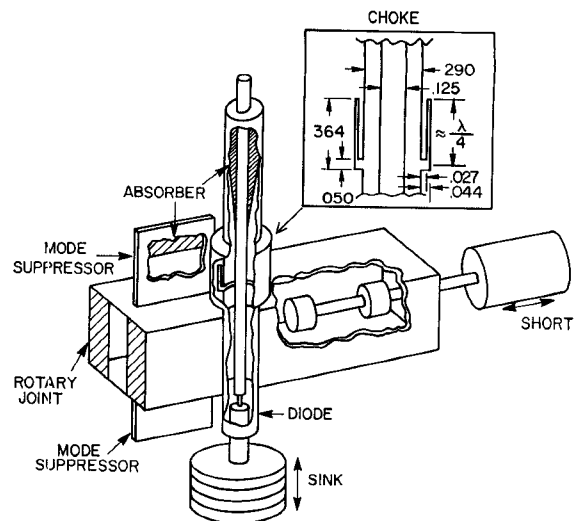


Fig. 1. Gunn oscillator circuit.

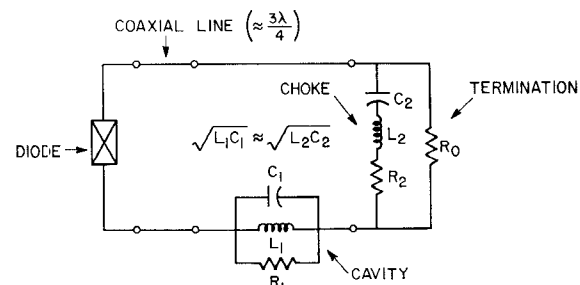


Fig. 2. Equivalent circuit.

broad walls of the cavity to eliminate mode probabilities (notably TE_{201}) other than the desirable TE_{101} [4].

Near cavity resonance, the equivalent circuit of the oscillator is shown in Fig. 2. With the reference plane located on the coaxial line at the center of the waveguide height, the loaded cavity is represented by a parallel resonant circuit. Without the choke in place the impedance versus frequency at this plane can be plotted on a Smith chart as a circular impedance locus which lies on the real axis between the center and right side of the chart. As seen from the diode position, this resonant loop can be positioned anywhere around the chart by varying the length of coaxial line between the diode and the cavity. The frequency of this resonance is easily varied by the waveguide short, while the diameter of the resonant loop is changed with the variable coupling between cavity and load. Thus almost any impedance value can be presented at the diode terminals in a predictable manner while properly terminating the diode at other frequencies. For diode impedance characterizations this tuning ability is sufficient.

For maximum output power under optimum tuning conditions, the wasted power due to the absorber in series with the cavity is unacceptable. By adding a choke in the coaxial line $\lambda/4$ from the effective cavity terminals, we can greatly reduce the termination resistance over a limited range of frequencies. In the case of IMPATT diodes, a choke is not necessary. The impedance of ordinary IMPATT diodes is quite small ($\approx 1 \Omega$); therefore, light cavity loading plus proper phasing gives the required impedance at the diode terminals, cavity impedance R_1 remains high compared to R_0 , and most of the power is coupled to the cavity. Gunn diodes, however, have a rather high impedance ($\approx 10 \Omega$); the cavity must be heavily loaded reducing R_1 so the choke is needed to reduce power loss to the termination R_0 . With the dimensions shown in the insert of Fig. 1, the choke has a Q of approximately 100, an effective series resistance of 7Ω , and the single-tuned behavior of the oscillator circuit is well preserved. The effect of the choke is clearly seen from Fig. 3, which shows the maximum output power versus frequency for a constant diode bias. At